

# Effects of short-range order on the electronic structure of disordered metallic systems

Derwyn A. Rowlands,<sup>1</sup> Julie B. Staunton,<sup>2</sup> Balazs L. Györfy,<sup>1</sup> Ezio Bruno,<sup>3</sup> and Beniamino Ginatempo<sup>3</sup>

<sup>1</sup>*H.H. Wills Physics Laboratory, University of Bristol, Bristol BS8 1TL, U.K.*

<sup>2</sup>*Dept. of Physics, University of Warwick, Coventry CV4 7AL, U.K.*

<sup>3</sup>*Dipartimento di Fisica, Università di Messina Salita Sperone 31, 98166 Messina, Italy*

(Dated: November 12, 2004)

For many years the Korringa-Kohn-Rostoker coherent-potential approximation (KKR-CPA) has been widely used to describe the electronic structure of disordered systems based upon a first-principles description of the crystal potential. However, as a single-site theory the KKR-CPA is unable to account for important environmental effects such as short-range order (SRO) in alloys and spin fluctuations in magnets, amongst others. Using the recently devised KKR-NLCPA (where NL stands for nonlocal), we show how to remedy this by presenting explicit calculations for the effects of SRO on the electronic structure of the *bcc*  $Cu_{50}Zn_{50}$  solid solution.

PACS numbers: 71.15.Ap, 71.23.-k, 71.20.Be, 71.15.mb

Currently, the first-principles theory of electrons in disordered metals is based upon Density Functional Theory (DFT) and either the Korringa-Kohn-Rostoker Coherent-Potential Approximation (KKR-CPA) [1] or its stripped down version, the LMTO-CPA [2], for averaging over the random configurations. This approach has been successfully applied to cases where the disorder is internal as well as external. Examples of the latter are metallic solid solutions such as  $Cu_cZn_{(1-c)}$  and  $Cu_cPd_{(1-c)}$  above their ordering temperatures  $T_0$ . Cases of the former are *Fe* or *Ni* above their Curie temperatures  $T_c$ , where randomness in the crystal potential seen by an electron is the consequence of Disordered Local Moments (DLM) [3], and valence fluctuating systems such as *Ce* [4]. Despite significant achievements [5], this methodology suffers from the shortcoming of not describing correlations in the fluctuations of the crystal potential. Evidently, as a single-site theory the CPA explicitly neglects such correlations. In this letter we present a generalization of the KKR-CPA theory which takes into account short-range order (SRO), and illustrate the new approach by quantitative calculations for the  $Cu_{50}Zn_{50}$  system.

The physics of the above SRO plays a particularly important role near phase transitions where it is frequently a precursor for long range order and can be said to be driving the ordering process. For example, in the ordering of the  $Cu_{50}Zn_{50}$  solid solution into an intermetallic compound of *B2* symmetry the system lowers its free energy by having unlike neighbours more frequently than like neighbours even in the disordered state, thereby lowering the temperature  $T_0$  where the system must finally order. Such SRO is also central to the understanding of electronic transport in general and in *K*-state alloys in particular [6]. Moreover, the formation of the moment in the DLM state of *Ni* [3], the creation of  $\gamma$ -like *Ce* atoms near the  $\gamma - \alpha$  transition [4], and also charge correlations (see [7] and references therein) and local lattice displacements in many alloys will be materially affected by their environment described by the SRO. The KKR-NLCPA

method [8, 9], to be summarised and illustrated here, will enable these important problems to be tackled in a parameter independent and material-specific way [10].

We begin by briefly summarising the derivation of the KKR-NLCPA [8, 9]. The first step is to define the scattering path matrix  $\hat{\tau}^{ij}$  describing the motion of an electron in an effective medium, which ideally should be determined so that it would describe the average properties of an electron exactly. It is a quantity which describes the full effects of the coherent potential and is given by

$$\hat{\tau}^{ij} = \hat{\underline{t}}\delta_{ij} + \sum_{k \neq i} \hat{\underline{t}} \left( \underline{G}(\mathbf{R}_{ik}) + \hat{\underline{\delta G}}(\mathbf{R}_{ik}) \right) \hat{\tau}^{kj}. \quad (1)$$

Here a circumflex symbol denotes an effective medium quantity and an underscore denotes a matrix in angular momentum space. In addition to effective local *t*-matrices  $\hat{\underline{t}}$  and the usual free-space KKR structure constants  $\underline{G}(\mathbf{R}_{ij})$  which account for the lattice structure, we also have effective structure constant corrections  $\hat{\underline{\delta G}}(\mathbf{R}_{ij})$  which take into account all nonlocal scattering correlations due to the disorder configurations (labelled  $\hat{\underline{\delta G}}^{ij}$  in Ref. [9]). Since the effective medium is translationally-invariant, the matrix elements  $\hat{\tau}^{ij}$  are also given by the Brillouin zone integral

$$\hat{\tau}^{ij} = \frac{1}{\Omega_{BZ}} \int_{\Omega_{BZ}} d\mathbf{k} \left( \hat{\underline{t}}^{-1} - \underline{G}(\mathbf{k}) - \hat{\underline{\delta G}}(\mathbf{k}) \right)^{-1} e^{i\mathbf{k}(\mathbf{R}_i - \mathbf{R}_j)}. \quad (2)$$

Since it is not feasible to solve the problem exactly, the key idea, based upon concepts from the Dynamical Cluster Approximation [11, 12], is to perform a consistent coarse-graining in both real and reciprocal space in order to appropriately deal with  $\hat{\underline{\delta G}}(\mathbf{R}_{ij})$  and  $\hat{\underline{\delta G}}(\mathbf{k})$  respectively. The construction for carrying out this coarse-graining, which must retain the translational invariance and point-group symmetry of the underlying lattice, has been given in Ref. [12] for a 2D square lattice in connection with a simple tight-binding model Hamiltonian. We have generalised this construction for realistic 3D lattices

[8] and implement it for the first time here. First we detail the construction for the body-centred cubic (*bcc*) lattice, the structure of disordered  $Cu_{50}Zn_{50}$ . Technically, the task is to find an appropriate set of  $N_c$  real-space cluster sites  $\{I, J\}$  and corresponding set of ‘cluster momenta’  $\{\mathbf{K}_n\}$  satisfying the relation

$$\frac{1}{N_c} \sum_{\mathbf{K}_n} e^{i\mathbf{K}_n(\mathbf{R}_I - \mathbf{R}_J)} = \delta_{IJ}. \quad (3)$$

This may be accomplished as follows:

1. Choose a real-space cluster of  $N_c$  sites such that the sites can be surrounded by a *tile* which a) preserves the point-group symmetry of the underlying lattice and b) can be periodically repeated to fill out all space. For  $N_c=1$ , the tiles are Wigner-Seitz cells surrounding each lattice point. For  $N_c>1$  there may only be solutions to the problem for particular values of  $N_c$  for any given lattice. For the *bcc* lattice the next allowed cluster sizes are  $N_c=2$  and  $N_c=16$ , where the tiles are simple cubes of volume  $a^3$  and  $(2a)^3$  respectively surrounding each cluster (see Fig. 1 for  $N_c=2$ ).

2. Label the sites of the original *bcc* lattice by the set of vectors  $\{\mathbf{R}_i^{bcc}\}$ , and the centres of the simple cubic coarse-graining tiles by the set of vectors  $\{\mathbf{R}_i^{sc}\}$ .

3. The reciprocal lattice corresponding to  $\{\mathbf{R}_i^{bcc}\}$  is a face-centred cubic (*fcc*) lattice made up of the reciprocal lattice vectors  $\{\mathbf{K}_i^{bcc}\}$ . Each  $\mathbf{K}_i^{bcc}$  is centred at a *fcc* Wigner-Seitz cell (or *bcc* Brillouin zone)  $\Omega_{BZ}^{bcc}$  of volume  $2(2\pi/a)^3$  which periodically repeat to fill out all of reciprocal space.

4. The coarse-grained system  $\{\mathbf{R}_i^{sc}\}$  has a simple cubic (*sc*) reciprocal lattice  $\{\mathbf{K}_i^{sc}\}$ , and each  $\mathbf{K}_i^{sc}$  is centred at a simple cubic tile of volume  $(2\pi/a)^3$  or  $(\pi/a)^3$  for the  $N_c=2$  or  $N_c=16$  cases respectively, which again periodically repeat to fill out all of reciprocal space. Note that  $\{\mathbf{K}_i^{bcc}\} \subset \{\mathbf{K}_i^{sc}\}$ .

5. Select  $N_c$  vectors from the set  $\{\mathbf{K}_i^{sc}\}$  which lie within  $\Omega_{BZ}^{bcc}$  and do not differ by an element of  $\{\mathbf{K}_i^{bcc}\}$ . We define these to be the set of cluster momenta  $\{\mathbf{K}_n\}$ . An example for  $N_c=2$  is shown in Fig. 1.

6. Finally, note that the reciprocal space contained within the  $N_c$  simple cubic tiles is completely equivalent to that contained within  $\Omega_{BZ}^{bcc}$  by translation through reciprocal lattice vectors  $\{\mathbf{K}_i^{bcc}\}$ .

Having carried out this coarse-graining procedure, we can now make an appropriate approximation to determine the effective medium. In reciprocal space, we approximate  $\widehat{\underline{G}}(\mathbf{k})$  by the set of  $N_c$  values  $\{\widehat{\underline{G}}(\mathbf{K}_n)\}$ , each defined to be the average of  $\widehat{\underline{G}}(\mathbf{k})$  over the tile centred at  $\mathbf{K}_n$ . The scattering path matrix may then be represented by the set of coarse-grained values

$$\widehat{\underline{t}}(\mathbf{K}_n) = \frac{N_c}{\Omega_{BZ}} \int_{\Omega_{\mathbf{K}_n}} d\mathbf{k} \left( \widehat{\underline{t}}^{-1} - \underline{G}(\mathbf{k}) - \widehat{\underline{G}}(\mathbf{K}_n) \right)^{-1}, \quad (4)$$

which are straightforward to calculate owing to  $\widehat{\underline{G}}(\mathbf{K}_n)$  being constant within each tile  $\Omega_{\mathbf{K}_n}$ . Note that the  $N_c$  integrals have the same total computational cost as one standard BZ integral. Using Eq. 3, the scattering path matrix at the cluster sites becomes

$$\widehat{\underline{t}}^{IJ} = \frac{1}{\Omega_{BZ}} \sum_{\mathbf{K}_n} \left( \int_{\Omega_{\mathbf{K}_n}} d\mathbf{k} \left( \widehat{\underline{t}}^{-1} - \underline{G}(\mathbf{k}) - \widehat{\underline{G}}(\mathbf{K}_n) \right)^{-1} \right) \times e^{i\mathbf{K}_n(\mathbf{R}_I - \mathbf{R}_J)} \quad (5)$$

From Nyquist’s sampling theorem [12], the effect of coarse-graining the effective structure constant corrections is to reduce their range in real space. In fact from Eq. 3 we have

$$\begin{aligned} \widehat{\underline{G}}(\mathbf{R}_{IJ}) &= \frac{1}{N_c} \sum_{\mathbf{K}_n} \widehat{\underline{G}}(\mathbf{K}_n) e^{i\mathbf{K}_n(\mathbf{R}_I - \mathbf{R}_J)} \\ \widehat{\underline{G}}(\mathbf{K}_n) &= \sum_{J \neq I} \widehat{\underline{G}}(\mathbf{R}_{IJ}) e^{-i\mathbf{K}_n(\mathbf{R}_I - \mathbf{R}_J)}. \end{aligned} \quad (6)$$

Note that  $\widehat{\underline{G}}(\mathbf{R}_{IJ})$  remains a translationally-invariant quantity which depends only on the distance between sites  $I$  and  $J$ , now within the range of the cluster size, but independent of which site in the lattice is chosen to be site  $I$  [8]. It is now straightforward to generalise the CPA argument and determine the medium by mapping to an impurity cluster problem. We choose a real-space cluster consistent with the requirements outlined above, and use the embedded cluster method [13] to replace it with an ‘impurity’ cluster of real *t*-matrices and free-space structure constants in the (still undetermined) effective medium. We then consider all paths starting and ending on the impurity cluster sites and demand that the average over the  $2^{N_c}$  possible impurity cluster configurations  $\gamma$  be equal to the path matrix for the effective medium itself i.e.

$$\sum_{\gamma} P(\gamma) \underline{t}_{\gamma}^{IJ} = \widehat{\underline{t}}^{IJ}, \quad (7)$$

where  $P(\gamma)$  is the probability of configuration  $\gamma$  occurring [14]. Therefore the effective medium *t*-matrices and effective structure constants are determined from a self-consistent solution of Eqs. 5 and 7. An example algorithm is given in Refs. [8, 9]. SRO may be included by appropriately weighting the configurations in Eq. 7 (the number of which can be reduced using symmetry and sampling), provided that translational-invariance is preserved. Observable quantities such as the density of states (DOS) can be calculated from the corresponding configurationally-averaged site-diagonal Green’s function [8, 9], which is independent of lattice site chosen. The formalism reduces to the KKR-CPA for  $N_c=1$ , and non-local scattering correlations (and SRO if desired) are systematically included into the effective medium as  $N_c$  is increased, becoming exact as  $N_c \rightarrow \infty$ .

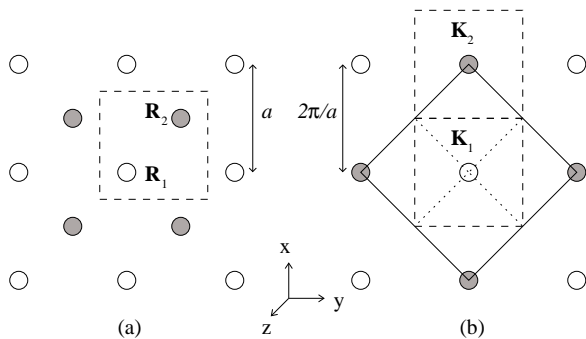


FIG. 1: (a) Cross-section of a real-space tile (dashed line) for a  $N_c=2$  cluster on the *bcc* lattice, with  $\mathbf{R}_1 = (0, 0, 0)$  and  $\mathbf{R}_2 = (a/2, a/2, a/2)$ , and the shaded sites lie out of the page. (b) Cross-section of the corresponding reciprocal-space tiles (dashed lines) for the  $N_c=2$  cluster, with  $\mathbf{K}_1 = (0, 0, 0)$  and  $\mathbf{K}_2 = (2\pi/a, 0, 0)$ , and the shaded points lie out of the page. The solid line denotes a cross-section of the first BZ in the  $(k_x, k_y)$  plane. The BZ can be visualised as a cube with a pyramid attached to each of the six faces, and the dotted line shows a projection of such a pyramid into the  $k_z$  plane.

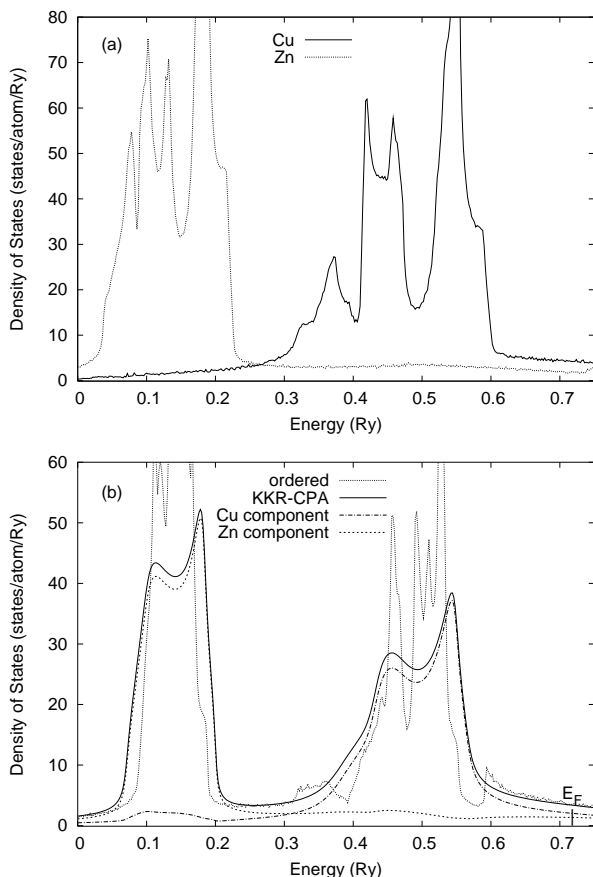


FIG. 2: (a) DOS for pure *Cu* and pure *Zn*. The energy contour has 1 mRy imaginary part. (b) DOS for both ordered and disordered (KKR-CPA)  $Cu_{50}Zn_{50}$ .  $E_F$  is the Fermi energy. Also shown are the component *Cu* and *Zn* plots for the disordered case.

To illustrate the ability of the KKR-NLCPA to describe the effects of SRO, we present calculations for the *bcc*  $Cu_{50}Zn_{50}$  solid solution with lattice constant 2.86Å. In all calculations that follow, *Cu* and *Zn* potentials come from self-consistent field (SCF) KKR-CPA calculations [15], and the BZ integrals use the adaptive quadrature method [16]. Fig. 2(a) shows DOS plots for pure *Cu* and pure *Zn*, and Fig. 2(b) shows a calculation for the ordered  $Cu_{50}Zn_{50}$  compound together with a KKR-CPA calculation for disordered  $Cu_{50}Zn_{50}$ . Since the energies of the *Cu* and *Zn* *d*-bands are very different, the system is said to be in the 'split band' regime. Physically, this means an electron travels more easily between *Cu* or between *Zn* sites than between unlike sites and so the decrease in overlap between like sites in the ordered case results in a narrowing of the *Cu* and *Zn* bands by a factor of two compared with the pure calculations [17]. For disordered  $Cu_{50}Zn_{50}$ , it is clear that the bands are widened and smoothed compared with the DOS for the ordered calculation. Also shown is the total DOS split into the component contributions from *Cu* and *Zn* impurity sites embedded in the KKR-CPA medium. Next, a KKR-NLCPA calculation for disordered  $Cu_{50}Zn_{50}$  for a two-site cluster ( $N_c=2$ ) is shown in Fig. 3(a). Although there is little observable difference in the total DOS compared with the KKR-CPA calculation (this difference shows up in detail only on a scale of  $\pm 1$  state/atom/Ry), the component contributions to the total DOS from the four possible cluster configurations are striking. (Although we find slightly more structure in the DOS for the larger  $N_c=16$  cluster, the results do not change by much in the absence of SRO). The component plots here are the DOS measured at the first cluster site when a particular cluster configuration is embedded in the KKR-NLCPA medium, which is the *Cu* site for the *Cu-Cu* and *Cu-Zn* configurations, and the *Zn* site for the *Zn-Cu* and *Zn-Zn* configurations. Crucially, owing to the translational invariance of the KKR-NLCPA medium, measurement at the second site gives the same results with a simple reversal of the labels of the *Cu-Zn* and *Zn-Cu* components. These component plots are particularly useful for interpreting the effects of SRO on the electronic structure, as we now show.

For  $N_c=2$ , it is possible to include SRO between nearest neighbour sites only. This is done by introducing the nearest neighbour Warren-Cowley SRO parameter  $\alpha$ , and using probabilities defined as  $P(CuCu)=P(Cu)^2+\alpha/4$ ,  $P(ZnZn)=P(Zn)^2+\alpha/4$ ,  $P(CuZn)=P(ZnCu)=P(Cu)P(Zn)-\alpha/4$  when averaging over the impurity cluster configurations in Eq. 7. For  $Cu_{50}Zn_{50}$ ,  $P(Cu)=P(Zn)=0.5$  and so the SRO parameter can take values in the range  $-1 \leq \alpha \leq 1$ , where -1, 0 and +1 correspond to ideal ordering, complete randomness, and complete clustering. Therefore as  $\alpha$  increases above zero, the probability of like pair components increases whilst that of unlike pairs decreases, becoming

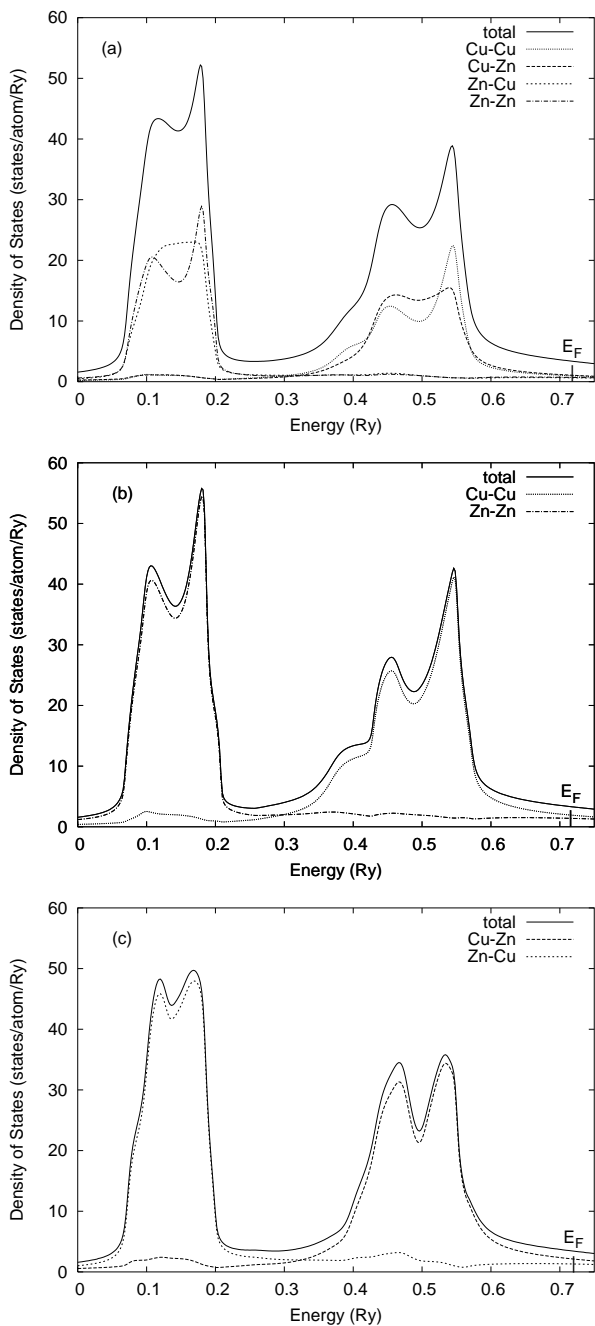


FIG. 3: (a) KKR-NLCPA calculation with  $N_c=2$  of the total and cluster component DOS for *bcc*  $Cu_{50}Zn_{50}$  with  $\alpha=0$ . (b) Same as (a) but with  $\alpha=+1$ , corresponding to short-range clustering. (c) Same as (a) but with  $\alpha=-1$ , corresponding to short-range ordering.  $E_F$  is the Fermi energy.

zero at  $\alpha=+1$ . As shown in Fig. 3(b), the total DOS is now completely dominated by the features of the *Cu-Cu* and *Zn-Zn* components. As expected these features are reminiscent of the pure bands shown in Fig. 2(a), for example the magnifying of the trough and peak either side of 0.15 Ry and 0.5 Ry can all be associated with the DOS for pure *Zn* and pure *Cu* respectively. More-

over, a new peak appears just before 0.4 Ry associated with pure *Cu*. On the other hand, as  $\alpha$  decreases below zero, the probability of like pairs decreases and becomes zero at  $\alpha=-1$ , as shown in Fig. 3(c). Evidently, for  $\alpha<0$  the DOS in general has a closer resemblance to that of ordered  $Cu_{50}Zn_{50}$  shown in Fig. 2(b). For example the peaks either side of 0.15 Ry and 0.5 Ry are now of roughly equal magnitude and there is also a slight overall narrowing of the bands compared with those for positive values of  $\alpha$  due to the decrease in probability of like neighbours.

In summary, we have generalised the KKR-CPA method to include SRO, and illustrated the dramatic changes that can occur in the DOS by application to the  $Cu_{50}Zn_{50}$  system. When combined with DFT (also enabling charge correlations and lattice displacements to be taken into account), the KKR-NLCPA will become part of a fully self-consistent theory in which the SRO parameter, determined via a linear response calculation [18], can be fed back into the electronic structure giving a completely parameter-free electronic description of the SRO at a given temperature  $T$ .

*Acknowledgments* Thanks to S. B. Dugdale and S. Ostantin for computational assistance. We acknowledge support from EPSRC (UK).

- 
- [1] B. L. Györfy, Phys. Rev. B **5**, 2382 (1972); G. M. Stocks *et al.*, Phys. Rev. Lett. **41**, 339 (1978).
  - [2] J. Kudrnovsky and V. Drchal, Phys. Rev. B **41**, 7515 (1990).
  - [3] J. B. Staunton and B. L. Györfy, Phys. Rev. Lett. **69**, 371 (1992).
  - [4] M. Lüders *et al.*, cond-mat/0406515 (2004).
  - [5] J. S. Faulkner, Prog. Mat. Sci. **27**, 1 (1982).
  - [6] H. Thomas, Z. Phys. **129**, 219 (1951).
  - [7] E. Bruno, L. Zingales, and Y. Wang, Phys. Rev. Lett. **91**, 166401 (2003).
  - [8] D. A. Rowlands, Ph.D. Thesis, Univ. of Warwick (2004).
  - [9] D. A. Rowlands, J. B. Staunton, and B. L. Györfy, Phys. Rev. B. **67**, 115109 (2003).
  - [10] The Cluster-CPA (S.S.A. Razee *et al.* Phys. Rev. B **42**, 9391, (1990)) is another self-consistent KKR cluster theory but has only been successfully applied to an s-phase-shift semicircular model for a pair cluster.
  - [11] M. H. Hettler *et al.*, Phys. Rev. B. **58**, 7475 (1998).
  - [12] M. Jarrell and H. R. Krishnamurthy, Phys. Rev. B **63**, 125102 (2001).
  - [13] A. Gonis *et al.*, Phys. Rev. B **29**, 555 (1984).
  - [14] The molecular CPA (M. Tsukada, J. Phys. Soc. Jpn **32**, 1475 (1972)) also has this self-consistency condition but the medium has an unphysical supercell structure.
  - [15] G. M. Stocks and H. Winter, Z. Phys. B **46**, 95 (1982); D. D. Johnson *et al.*, Phys. Rev. Lett **56**, 2088 (1986).
  - [16] E. Bruno and B. Ginatempo, Phys. Rev. B. **55**, 12946 (1997).
  - [17] V. L. Moruzzi *et al.*, Phys. Rev. B. **9**, 3316 (1974).
  - [18] J. B. Staunton *et al.*, Phys. Rev. B. **50**, 1450 (1994).